May 2008

SLAC-PUB-13222

Identification of the Origin of Monojet Signatures at the LHC * †

Thomas G. Rizzo

Stanford Linear Accelerator Center, 2575 Sand Hill Rd., Menlo Park, CA, 94025

Abstract

Several new physics scenarios can lead to monojet signatures at the LHC. If such events are observed above the Standard Model background it will be important to identify their origin. In this paper we compare and contrast these signatures as produced in two very different pictures: vector or scalar unparticle production in the scale-invariant/conformal regime and graviton emission in the Arkani-Hamed, Dimopoulos and Dvali extra-dimensional model. We demonstrate that these two scenarios can be distinguished at the LHC for a reasonable range of model parameters through the shape of their respective monojet and/or missing E_T distributions.

Submitted to Physics Letters B

*Work supported in part by the Department of Energy, Contract DE-AC02-76SF00515
†e-mail: rizzo@slac.stanford.edu

1 Introduction and Background

The LHC will turn on during 2008 and it is generally expected that new physics beyond the Standard Model(SM) will be discovered at some point thereafter once significant luminosity is accumulated and the the two detectors are sufficiently well-understood. What new physics signatures will be observed and how will they be grounded within a specific theoretical framework? Clearly once the new physics is found, our primary goal will be to uncover its origin and to identify the underlying model which generates it. This can sometimes be confusing as in many cases several kinds of new physics can lead to quite similar signatures at colliders. Supersymmetry[1] and Universal Extra Dimensions[2] provide us with one well-known example of this possible model confusion which has been much discussed in the recent literature[3]. The ability of the LHC to differentiate models with similar signatures may become the the most important issue once new physics is discovered.

In this paper we will consider another example of this kind of potential confusion which may arise at the LHC between two very different scenarios: graviton emission in the extra-dimensional model of Arkani-Hamed, Dimopoulos and Dvali(ADD)[4] and the production of scalar/vector unparticles in the model of Georgi[5] in the scale-invariant/conformal regime[6] where the unparticle can be treated as both 'massless' and stable. Here, by a 'massless' unparticle we will mean one that has a null threshold mass parameter, *i.e.*, $\mu^2 = 0$, which determines the *minimum* allowed value of its possible squared 4-momentum[6], *i.e.*, $\mu^2 \leq P^2$. (Recall that for unparticles the value of P^2 actually takes on a continuous range which is integrated over to obtain observable cross sections.) Both of these new physics models can lead to a monojet signal, *i.e.*, a single jet plus missing E_T (MET) with balancing transverse momenta, at the LHC. In the ADD case, this scenario has been studied in some detail in the classic work by Vacavant and Hinchliffe[7] within the ATLAS[8] setting, which we will use as a guide for the present analysis.[‡] Assuming that monojet signals above the SM backgrounds are indeed observed at the LHC we will demonstrate that the shapes of the

[‡]CMS[9] has also performed a more recent but comparable analysis in the single photon channel.

corresponding excess jet and/or missing E_T distributions are qualitatively quite distinctive in these two cases. This will allow these two classes of models to be distinguished at the LHC for a range of parameters provided that sufficient integrated luminosity is available.

As emphasized by Vacavant and Hinchliffe[7], observing an excess in the monojet channel relies on our thorough understanding of the SM background. At low E_T, this background can be dominated by QCD/jet energy mis-measurements. However, at high E_T it is largely dominated by $Z + j$ production followed by the decay $Z \to \nu\bar{\nu}$. Fortunately, in practice, it appears that neither ATLAS nor CMS[10] will need to rely solely on Monte Carlo estimates to fully understand this MET plus jet(s) background. At high E_T one can instead employ the 'standard candle' approach where one makes use of the same production channel but now with the Z decaying leptonically, *i.e.*, $Z \to e^+e^-/\mu^+\mu^-$. These easily measured rates can then be corrected for differences in the branching fractions as well as for acceptances and efficiencies to obtain the Z-induced SM monojet background[11] directly from data. In the analysis presented below we will assume that this procedure works so that this background will eventually be well understood in the very high E_T region above 500 GeV, corresponding to an $M_{eff} = E_{T_j} + \text{MET} \geq 1$ TeV upon which we will concentrate. We will not include in the present analysis possible additional information that may be obtainable from the lower E_T region where the jet energy mis-measurements can be a potentially large source of SM backgrounds. The resulting SM background estimates that we obtain and will employ below are found to be essentially the same as, though perhaps $10 - 20\%$ larger than, those found by Vacavant and Hinchliffe[7].

Our procedure is rather straightforward: First, we will demonstrate that the overall *shape* of the normalized monojet E_T distribution predicted by the ADD model is essentially independent of the number of extra dimensions in the relevant parameter range. Next we will show that the predictions for the corresponding normalized monojet E_T spectra produced by either scalar and vector unparticles lie in a rather narrow band. By comparing these two sets of distributions it will then become clear that for sufficiently high integrated luminosities, $\sim 100 fb^{-1}$, these two

predictions will be easily isolated from one another in E_T space so that we can distinguish these two classes of models at the LHC by using the data collected above $E_T = 500$ GeV.

2 Analysis

Let us begin by considering the monojet signal[12] in the ADD model which arises from graviton Kaluza-Klein tower (G) emission in the following processes: $q\bar{q} \to gG$, $gg \to gG$ and $q(\bar{q})g \to q(\bar{q})G$. The expressions for these parton-level cross sections are given in full detail in Ref.[12]. In the original ADD scenario, the resulting cross section expressions depend upon only 2 parameters: the number of extra dimensions, $2 \leq \delta \leq 7$, and the value of the $D = 4 + \delta$-dimensional Planck scale, M_D; these subprocess level cross sections are observed to scale as $\sim M_D^{-(2+\delta)}$. Since the ADD model is only an effective theory below the mass scale M_D, in performing the integrations necessary to obtain the relevant LHC cross sections it is unclear how to treat the kinematic region where the partonic center of mass energy, $\hat{s}$, is in excess of M_D. There are two common ways that one can address this issue discussed in the literature[7, 12]. First, we could simply ignore this problem and perform the necessary integration; a second possibility is to make a hard truncation in the integration at $\hat{s} = M_D^2$. The former choice will, of course, lead to a larger event rate but one finds that these two approaches yield qualitatively similar but quantitatively different numerical results. In performing our analysis, we will instead follow an intermediate approach and employ a gravitational form factor[13] which naturally controls the large $\hat{s}$ part of the cross section, extending the range of validity of the partonic cross section above $\hat{s} = M_D^2$ and maintains unitarity at high energies. For numerical purposes we will use a fixed form factor scale of $\Lambda_{FF} = 8$ TeV in this analysis. One finds, however,that varying this particular choice makes little numerical difference in the results presented below, as an explicit examination reveals, since the form factor only leads to modifications in the extreme high end of the various E_T distributions where there are very limited statistics.

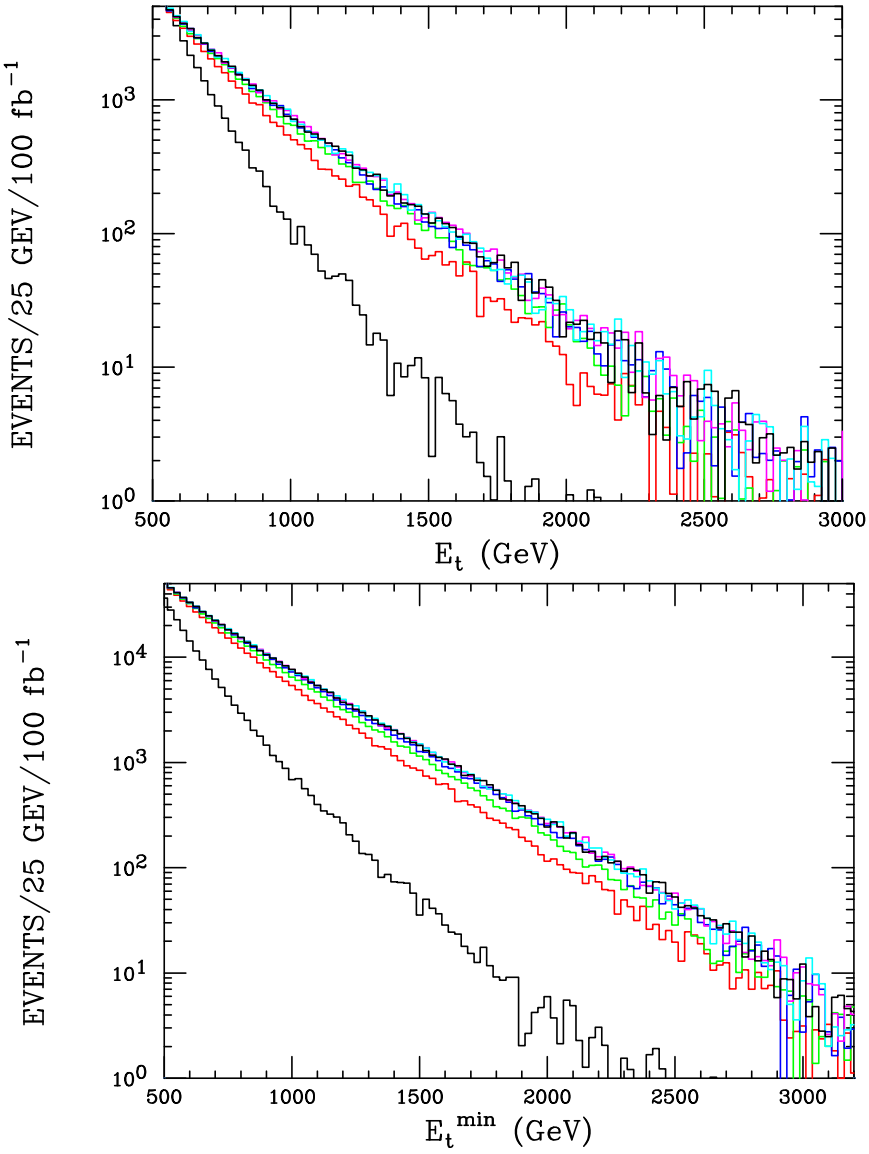

Figure 1: Event rate for the monojet signal induced by graviton emission in the ADD model assuming $2 \leq \delta \leq 7$, from bottom to top, as a function of the jet E_T in the top panel or above a minimum jet E_T cut in the lower panel. Note that a cut on the jet rapidity of $|\eta_j| \leq 3$ has been applied in all cases. As discussed in the text the values of M_D have been adjusted in each case so as to give the same prediction as that for $M_D = 4$ TeV with $\delta = 2$ at an E_T value of 500 GeV. Note that for comparison purposes these ADD predictions are for pure signal *only*. The SM background is represented in either panel by the lowest black histogram.

Since our goal is to differentiate monojet signals arising in different models by the *shapes* of their jet E_T distributions, it is instructive to first compare the ADD model 'with itself', *i.e.*, to compare the ADD predictions for different values of δ while simultaneously varying the value of M_D (as a function of δ) so that the models all predict the same cross section at some fixed value of the jet E_T. This allows us to directly compare the predicted shape for the signal monojet spectrum for each value of δ without having to worry about the overall normalization of the spectrum. Note that in all cases the subprocess cross sections for graviton emission are seen to grow rapidly with $\hat{s}$ and so can naturally lead to large event excesses at high E_T. As an example, let us assume a reference value for the monojet cross section corresponding to the choice of $\delta = 2$ with $M_D = 4$ TeV. For all larger values of δ we will then adjust the associated value of M_D such that identical cross sections are obtained when evaluated at a jet energy of $E_T = 500$ GeV. Note that there is nothing particularly special about this choice of E_T value other than it allows us to have a reasonable signal-to-background ratio for all values of δ for the integrated luminosities that we will assume in our analysis. Other choices for this cross-over point in the ADD case would yield qualitatively similar results since we are only probing the various shapes of the E_T distributions here. We next determine the resulting LHC monojet event rates for each case as a function of jet E_T while simultaneously demanding that the monojet be more or less central in rapidity, *i.e.*, $|\eta_j| \leq 3$, as assumed by Vacavant and Hinchliffe[7]; to be specific, we employ the CTEQ6.6M PDFs[14] throughout and will assume a fixed integrated luminosity of 100 fb^{-1}. In a similar manner, we can also ask for the cumulative number of events *above* a minimum cut on the jet E_T which probes a somewhat different aspect of the jet E_T spectrum. As we will see, the additional statistics in this distribution will allow for an improved separation of models.

The results of this analysis together with an estimate of the SM $Z + j$ induced backgrounds are shown in Fig. 1 for $2 \leq \delta \leq 7$ assuming jet E_T's larger than 500 GeV. Here we see that while the ADD model for the chosen set of parameter ranges clearly produces a significant signal above the SM background it is very difficult to determine the value of δ itself since all of the predicted

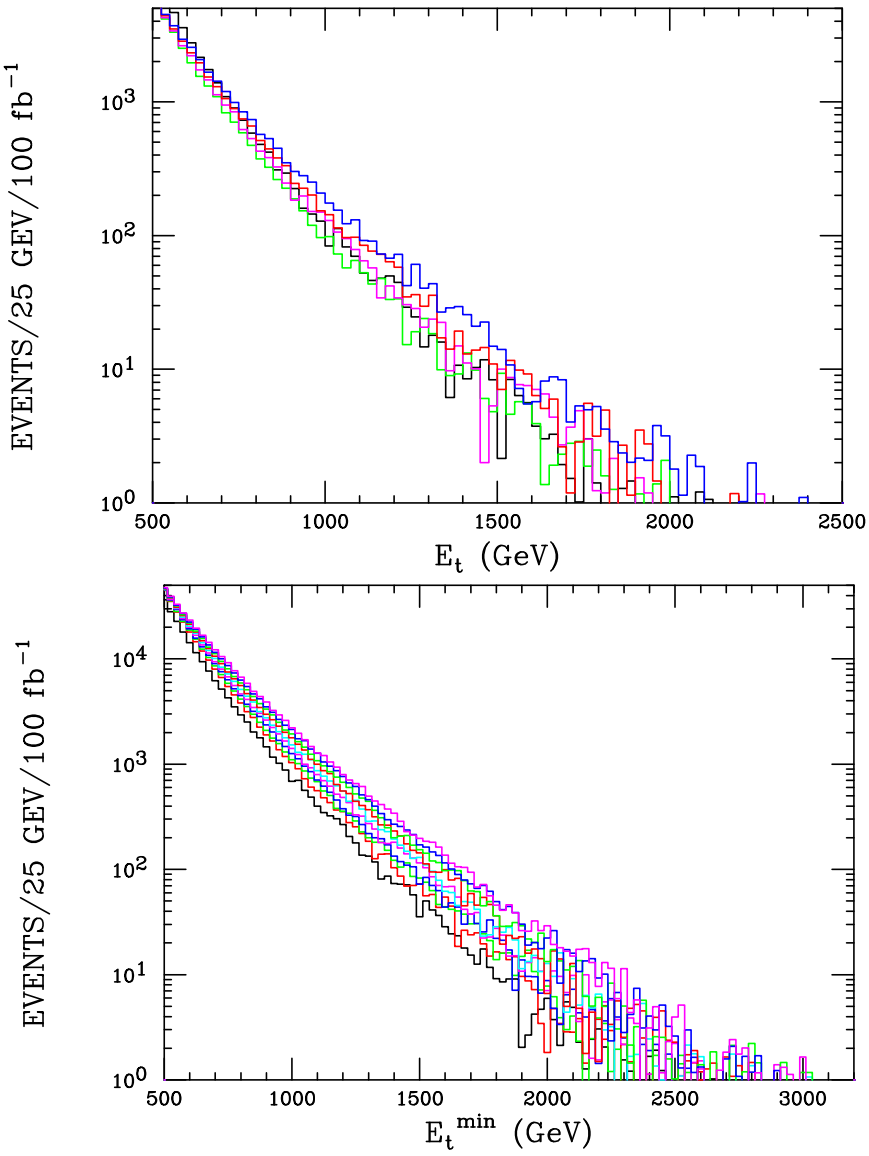

Figure 2: Same as Fig.1, but now for vector unparticles with, from bottom to top, $d = 1.1$ to $d = 1.9$ in steps of 0.1(0.2) in the lower(upper) panel.

distributions lie rather close to one another[§]. This is seen to be an even stronger conclusion for the case of the E_T^{cut} distributions. This reproduces the well-known result[7] that at the LHC it is essentially impossible, or at least extremely difficult, to determine both the values of M_D and δ simultaneously from the observation of a monojet excess at a *fixed* value of $\sqrt{s}$. However, for our purposes, this is a *positive* result since our goal is to distinguish the set of *all* ADD predictions from those of other models, specifically, those arising from unparticles. The ADD prediction for the shape of these E_T and E_T^{cut} distributions are thus found not to be very sensitive to the specific value of δ, especially when $3 \leq \delta$. Note that if the value of $E_T = 500$ GeV, chosen as the cross-over point where the various ADD predictions yield the same cross section, was taken to be somewhat larger then any determination of the value of δ would be only be made more difficult since the divergences in the observed spectra would be reduced. Lowering the cross-over point would increase the lever arm somewhat but, as we can easily see from this figure, would at most only be useful in separating the $\delta = 2$ case from the other choices for δ.

When considering the predictions of the unparticle model, with which we wish to compare the ADD scenario, the parameter space is somewhat more varied and there are many possibilities. Here, to be specific, we will consider the case of 'massless' unparticles, as described above, which are assumed to be either scalar (spin-0), U_S, or vector (spin-1), U_V, and in either case are sufficiently stable so that they can lead to a collider missing E_T signature. However, we have checked that by adding a small unparticle threshold mass, $\mu \lesssim 100$ GeV, so that $P^2 \geq \mu^2$, we will not significantly alter the numerical results presented below as long as the relative stability of the unparticle on collider scales is also maintained. This is clear since for these $2 \to 2$ processes small threshold masses for the unparticles will only result in a small reduction in the size of the relevant phase space which is of order $\sim \mu^2/\hat{s}$. Having made these particular choices, several other parameter options still can remain. If we take the simplest possibility and assume that the unparticle couples as a SM gauge singlet to only one operator constructed of only single type of SM field, then the

[§]The results for $\delta = 2$ are seen to lie slightly below the others so that this case may be confidently distinguished from the others at somewhat higher integrated luminosities. It is important to note, however, that the predictions for larger values of δ lead to slightly harder distributions.

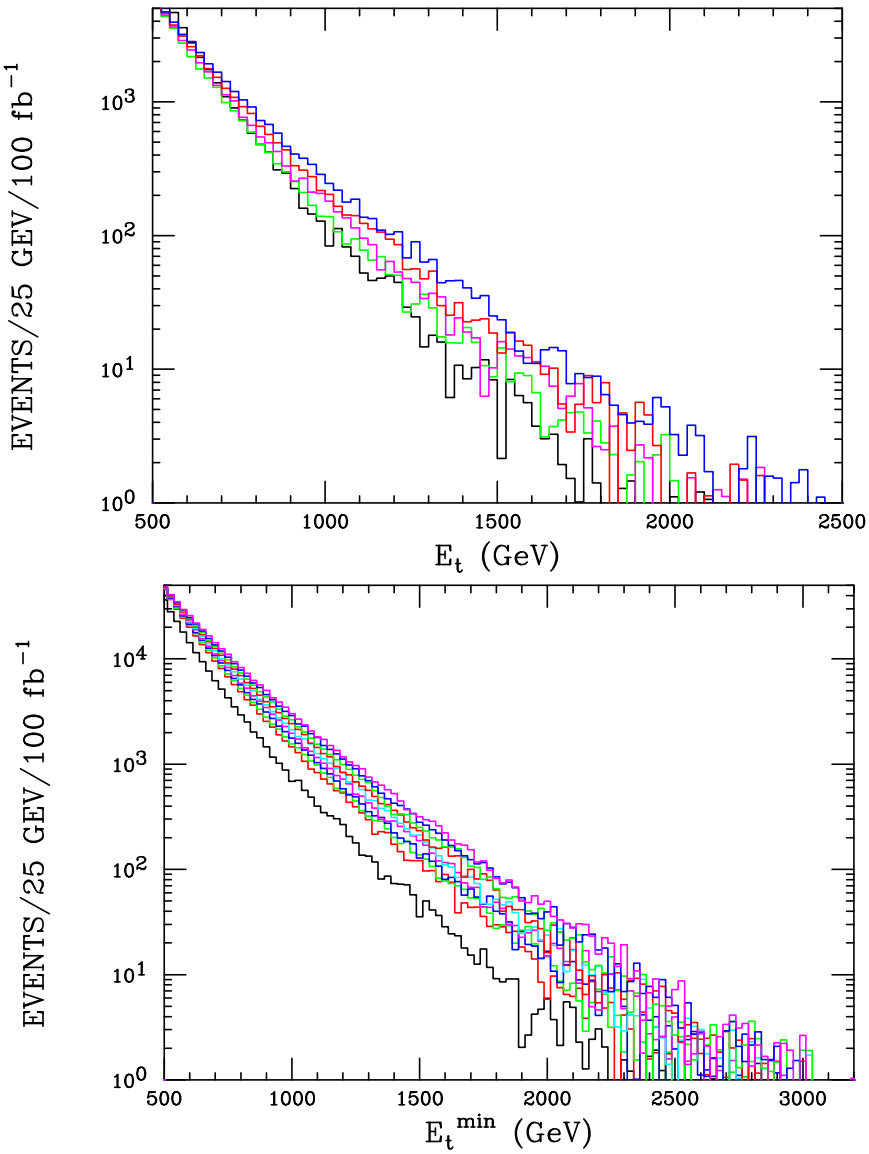

Figure 3: Same as Fig.1, but now for $r = 0$ scalar unparticles with, from bottom to top, $d = 1.1$ to $d = 1.9$ in steps of 0.1(0.2) in the lower(upper) panel.

resulting interaction will depend upon only an overall scale, Λ, as well as the value of the effective unparticle anomalous dimension, d, which is restricted to lie in the range $1 < d < 2$. If, however, the unparticle is allowed to couple to several different SM operators, then the relative strengths of these interactions, r_i, can also become quite relevant. Here, to be specific, we will assume that the spin-0 unparticles couple to the relevant SM fields via

$$\frac{1}{\Lambda^{d-1}} \sum_q \bar{q} q U_S + r \frac{1}{\Lambda^d} G^a_{\mu\nu} G^{\mu\nu}_a U_S \,, \tag{1}$$

for all quark fields q and where $G^a_{\mu\nu}$ is the gluon field strength tensor; we will consider the two cases $r = 0, 1$ below as representative examples. We will further assume that the spin-1 unparticles couple only to the SM quarks via

$$\frac{1}{\Lambda^{d-1}} \sum_q \bar{q} \gamma_\mu q U^\mu_V \,, \tag{2}$$

also in a universal manner. The parton-level cross sections for the relevant processes $q\bar{q} \to g U_V$, $q(\bar{q})g \to q(\bar{q}) U_V$ and $gg \to g U_S$ can be found in Ref.[15]. Correspondingly, we find that the (reduced) spin and color-averaged squared matrix elements for the remaining processes of interest are given, in a slightly modified version of the notation of Ref.[15], by

$$\begin{aligned} |\bar{M}|^2(q\bar{q} \to g U_S) &= \frac{16\pi\alpha_s}{9\hat{u}\hat{t}\Lambda^2}(\hat{s}^2 - (P^2)^2) \\ |\bar{M}|^2(qg \to q U_S) &= \frac{2\pi\alpha_s}{-3\hat{u}\hat{s}\Lambda^2}(\hat{t}^2 - (P^2)^2) \,, \end{aligned} \tag{3}$$

where P^2 is the unparticle invariant mass, as defined above, which is integrated over to obtain a final cross section result. A similar expression is found to hold in the case of the $\bar{q}g$ initial state. The corresponding differential cross sections are then given by

$$\frac{d^2\sigma}{d\hat{t} dP^2} = \frac{1}{16\pi\hat{s}^2} \frac{A_d}{2\pi} |\bar{M}|^2 \Big(\frac{P^2}{\Lambda^2}\Big)^{d-2} \,, \tag{4}$$

where $\hat{t}$ is the usual subprocess-level Mandelstam variable and A_d is the familiar unparticle numerical phase space factor as given by Georgi[5]. It is interesting to note that the scaling behavior of the unparticle cross sections for both the unparticle vectors and $r = 0, 1$ scalars is such that they will lead to essentially the same E_T dependence as the SM background in the limit when $d \to 1$. This is not surprising since in that limit the unparticles behave in a manner similar to the more conventional SM boson fields. In keeping with the ADD distribution shape analysis above, we will in all cases adjust the value of the scale Λ so that the unparticle monojet cross section at $E_T = 500$ GeV is the same as that for the ADD model with $M_D = 4$ TeV with $\delta = 2$ at the same E_T. In order to do this it is obvious that different values of Λ will need to be chosen as both d and r are varied for both the scalar and vector unparticle cases independently.

Figs. 2, 3 and 4 show the results analogous to Fig. 1 for the vector unparticle as well as the scalar unparticle cases with $r = 0, 1$, respectively. Several things are immediately obvious from these figures. First, as expected, the overall shape of the unparticle E_T and E_T^{cut} spectra becomes stiffer as the value of d is increased. This is not too surprising as the leading subprocess cross sections are observed to scale as $\sim (\hat{s}/\Lambda^2)^{d-1}$ relative to the $Z + jet$ SM background. Secondly, the distributions we obtain for both the scalar and vector particles are, for the same value of d, essentially of the same shape. Again, this is not surprising as these two case differ only in the tensor structure of the unparticle interaction. The $r = 0$ and $r = 1$ scalar interactions are slightly different due to the additional unparticle coupling to the gluon. While this operator is suppressed by an additional power of $\hat{s}/\Lambda^2$, the initial state gg luminosity at relatively low E_T is very large and somewhat offsets this suppression. All in all, the predictions for the monojet spectra of these representative unparticle models are found to lie in a somewhat narrow band which is observed to be harder at high E_T and E_T^{cut} than is the SM background.

Up to now we have found that both the ADD predictions for the monojet E_T and E_T^{cut} spectra and those from unparticles separately lie in rather restricted ranges. How do these ranges compare? Since the hardest E_T spectrum in the unparticle model is obtained for large d and the

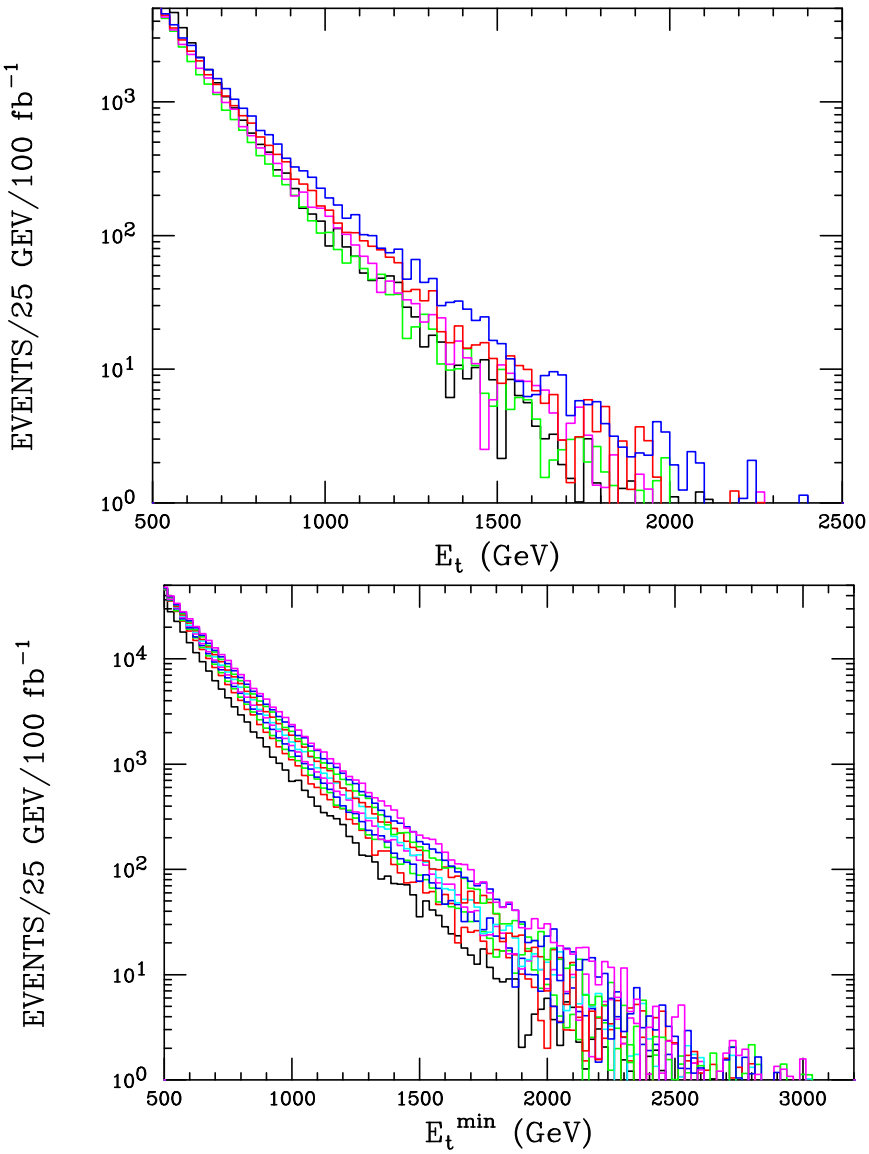

Figure 4: Same as Fig.1, but now for $r = 1$ scalar unparticles with, from bottom to top, $d = 1.1$ to $d = 1.9$ in steps of 0.1(0.2) in the lower(upper) panel.

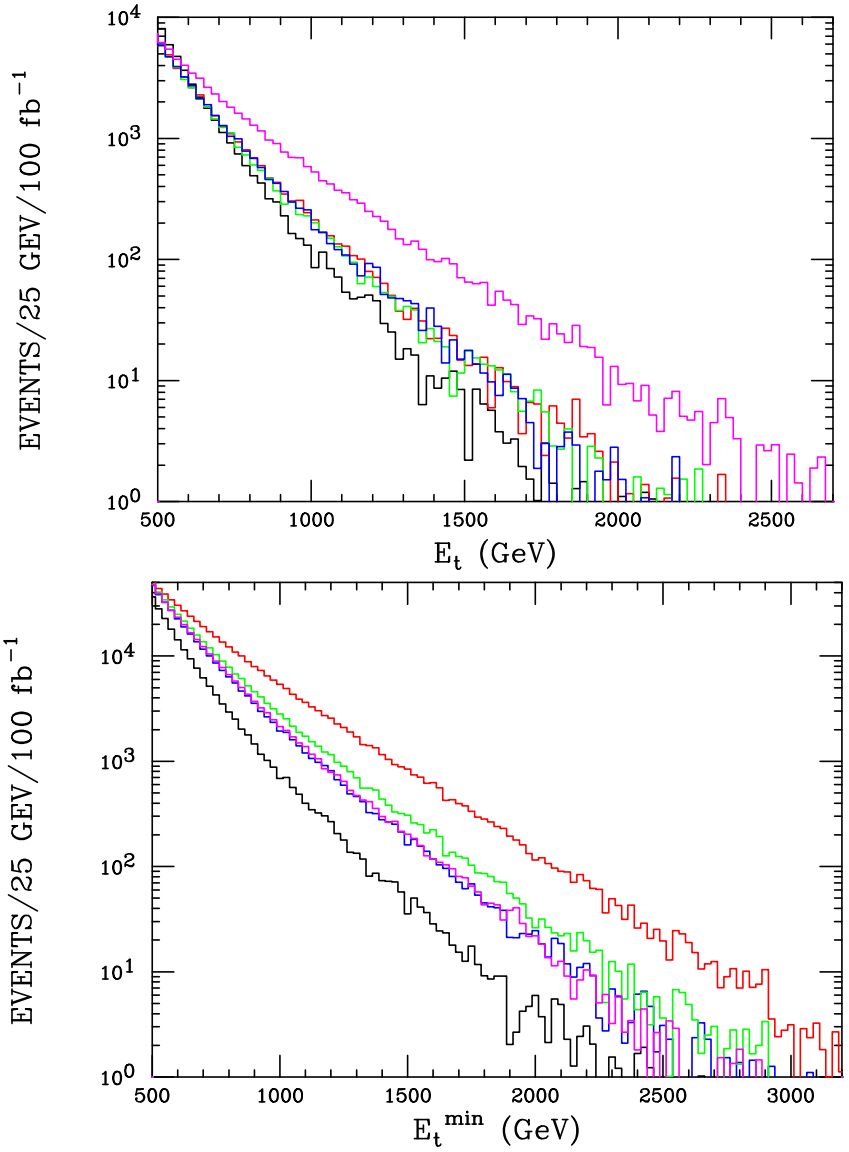

Figure 5: Sample comparison of the predictions for the monojet E_T and E_T^{cut} distributions in the ADD model with $M_D = 4$ TeV and $\delta = 2$ (upper red histogram) with the case of vector and scalar unparticles (with either $r = 0, 1$) assuming $d = 1.8$. Also shown is the SM background (black histogram).

softest spectrum for ADD occurs when $\delta = 2$ it is most instructive to compare these specific two cases. Any other pair of spectra will clearly lie further apart in E_T space and so will be more easily distinguished. Fig. 5 shows a representative set of comparisons of these two cases taking the above observations into account. Here we see that the three sample unparticle model predictions are relatively clustered together and lie in between those for the ADD scenario and the SM background. While the unparticle predictions themselves are difficult to distinguish it is clear that they are all easily differentiable from those of the ADD model. It is clear that a very large amount of jet energy smearing would be necessary to make these two predicted E_T regions appear to overlap to any extent. These results demonstrate that with enough statistics the shapes of the excess monojet E_T distributions arising from these two classes of models can be distinguished at the LHC provided that they are visible above the SM background. We would, however, hope that a more detailed study by ATLAS/CMS using a full detector simulation will be performed to verify these results.

3 Discussion and Conclusions

In this paper we have explored the capability of the high luminosity LHC to differentiate two sets of new physics models that can lead to visible missing E_T/monojet signatures. The relevant tools for model discrimination are the shapes of the resulting monojet E_T and E_T^{cut} distributions themselves. First, we demonstrated that (i) the predictions of the ADD for the monojet E_T/E_T^{cut} distributions form a very narrow band for $2 \leq \delta \leq 7$ and, (ii) Similarly, the corresponding predictions in the case of vector or scalar unparticles also so lie in a different but not so narrow band. Second, we showed that these two bands are seen not to overlap when integrated luminosities of order $\sim 100 fb^{-1}$ are available implying that these two classes of models which induce the monojet signal can be distinguished at the LHC.

References

[1] For a phenomenological introduction to SUSY, see H. Baer and X. Tata, *Weak scale supersymmetry: From superfields to scattering events*, *Cambridge, UK: Univ. Pr. (2006) 537 p*; M. Drees, R. Godbole and P. Roy, *Theory and phenomenology of sparticles: An account of four-dimensional N=1 supersymmetry in high energy physics*, *Hackensack, USA: World Scientific (2004) 555 p.*

[2] T. Appelquist, H. C. Cheng and B. A. Dobrescu, Phys. Rev. D **64**, 035002 (2001) [arXiv:hep-ph/0012100].

[3] There has been much work on this subject; see for example, A. Datta, K. Kong and K. T. Matchev, Phys. Rev. D **72**, 096006 (2005) [Erratum-ibid. D **72**, 119901 (2005)] [arXiv:hep-ph/0509246]; C. Athanasiou, C. G. Lester, J. M. Smillie and B. R. Webber, JHEP **0608**, 055 (2006) [arXiv:hep-ph/0605286]; L. T. Wang and I. Yavin, JHEP **0704**, 032 (2007) [arXiv:hep-ph/0605296]; J. M. Smillie, Eur. Phys. J. C **51**, 933 (2007) [arXiv:hep-ph/0609296]; S. Y. Choi, K. Hagiwara, H. U. Martyn, K. Mawatari and P. M. Zerwas, Eur. Phys. J. C **51**, 753 (2007) [arXiv:hep-ph/0612301]; C. Kilic, L. T. Wang and I. Yavin, JHEP **0705**, 052 (2007) [arXiv:hep-ph/0703085]; C. Csaki, J. Heinonen and M. Perelstein, JHEP **0710**, 107 (2007) [arXiv:0707.0014 [hep-ph]]; L. T. Wang and I. Yavin, arXiv:0802.2726 [hep-ph].

[4] N. Arkani-Hamed, S. Dimopoulos and G. R. Dvali, Phys. Lett. B **429**, 263 (1998) [arXiv:hep-ph/9803315].

[5] H. Georgi, Phys. Lett. B **650**, 275 (2007) [arXiv:0704.2457 [hep-ph]] and H. Georgi, Phys. Rev. Lett. **98**, 221601 (2007) [arXiv:hep-ph/0703260].

[6] See for example P. J. Fox, A. Rajaraman and Y. Shirman, Phys. Rev. D **76**, 075004 (2007) [arXiv:0705.3092 [hep-ph]]; A. Delgado, J. R. Espinosa and M. Quiros, JHEP **0710**, 094 (2007) [arXiv:0707.4309 [hep-ph]]; M. J. Strassler, arXiv:0801.0629 [hep-ph]; V. Barger, Y. Gao,

W. Y. Keung, D. Marfatia and V. N. Senoguz, Phys. Lett. B **661**, 276 (2008) [arXiv:0801.3771 [hep-ph]].

[7] L. Vacavant and I. Hinchliffe, J. Phys. G **27**, 1839 (2001).

[8] ATLAS Detector and Physics Performance Technical Design Report, http://atlas.web.cern.ch/Atlas/GROUPS/PHYSICS/TDR/access.html.

[9] CMS Physics Technical Design Report, https://cmsdoc.cern.ch/cms/cpt/tdr/ and G. L. Bayatian *et al.* [CMS Collaboration], J. Phys. G **34**, 995 (2007).

[10] For a discussion, see M. Spiropulu, arXiv:0801.0318 [hep-ex]; C. Buttar *et al.*, arXiv:0803.0678 [hep-ph]; M. Tytgat, arXiv:0710.1013 [hep-ex]; A. Tricomi, talk given at HEP2007, Manchester, England, 19-25 July 2007; G.Polesello and V. Zhuravlov, talks give at the *'Physics at the Terascale' Workshop*, DESY, 03-05 December 2007; R. Cavanaugh, talk given at the 2008 Aspen Winter Conference, 13-19 January 2008; S. Tsuno, talk given at Moriond Electroweak 2008, La Thuile, Italy, 01-08 March 2008; A. De Roeck, talk given at *Physics of the Large Hadron Collider* Workshop, Kavli Institute, UCSB, 01 April 2008.

[11] This method has already been used successfully at the Tevatron: A. Abulencia *et al.* [CDF Collaboration], Phys. Rev. Lett. **97**, 171802 (2006) [arXiv:hep-ex/0605101]; V. M. Abazov *et al.* [D0 Collaboration], Phys. Rev. Lett. **90**, 251802 (2003) [arXiv:hep-ex/0302014].

[12] G. F. Giudice, R. Rattazzi and J. D. Wells, Nucl. Phys. B **544**, 3 (1999) [arXiv:hep-ph/9811291].

[13] J. Hewett and T. Rizzo, JHEP **0712**, 009 (2007) [arXiv:0707.3182 [hep-ph]]; see also D. F. Litim and T. Plehn, arXiv:0707.3983 [hep-ph].

[14] P. M. Nadolsky *et al.*, arXiv:0802.0007 [hep-ph].

[15] K. Cheung, W. Y. Keung and T. C. Yuan, Phys. Rev. D **76**, 055003 (2007) [arXiv:0706.3155 [hep-ph]] and Phys. Rev. Lett. **99**, 051803 (2007) [arXiv:0704.2588 [hep-ph]].